2010 American Control Conference
Marriott Waterfront, Baltimore, MD, USA
June 30-July 02, 2010

$\mathcal{H}_\infty$ Performance and Robust Topology Design of Relative Sensing Networks

Daniel Zelazo[†] and Mehran Mesbahi[‡]

Abstract— **This work provides a general framework for the analysis and synthesis of a class of relative sensing networks (RSN) in the context of its $\mathcal{H}_\infty$ performance. In an RSN, the underlying connection topology couples each agent at their outputs. A distinction is made between RSN with homogeneous agent dynamics and RSN with heterogeneous dynamics. In both cases, explicit graph theoretic expressions and bounds for the $\mathcal{H}_\infty$ performance are derived. The $\mathcal{H}_\infty$ performance is structure dependent and related to the spectral radius of the graph Laplacian. The analysis results are then used to develop synthesis methods for RSNs. Using results from robust semi-definite programming, a synthesis procedure for the design of a robust sensing topology is derived.**

I. INTRODUCTION

Many applications in multi-agent systems rely on relative sensing to achieve their team objectives. For example, space applications relying on relative sensing include spacecraft constellations for studying the structure of the heliopause, stereographic imaging and tomography for space physics, and space borne optical interferometry for probing the origins of the cosmos and identifying Earth-like planets (e.g., TPF, MAXIM) [6], [9], [15], [21]. Distributed sensor networks also rely on relative sensing and include applications ranging from environmental surveillance, modeling, localization, and collaborative information processing [1], [2], [3], [17].

Fundamental to all these systems is the implicit presence of a "network." The exchange of information between each agent in a relative sensing network describes an underlying connection topology, which can have profound implications on the performance and design of decentralized schemes for estimation and control. As a result, it is becoming more important to examine notions of systems performance from the perspective of the underlying connection topology describing the interactions of each agent. Recent examples of such graph-centric analysis include relating closed-loop stability properties of multi-agent systems to the spectral properties of the graph Laplacian [8], relating controllability in consensus seeking systems to graph symmetry [19], graph-theoretic analysis and performance bounds for consensus systems [5], [23], and graph-centric observability properties of relative sensing networks [22], [20].

In this work we focus on systems that rely on relative sensing to achieve their mission objectives. We refer to this class of systems as Relative Sensing Networks (RSN). In RSNs, the underlying connection topology couples the agents at their outputs. Such systems are prevalent in formation flying applications where relative sensing is employed to measure inter-agent distances [16], [12]. More fundamentally, these types of networks are relevant for applications involving distributed sensing for purposes of estimation and control.

Th paper is an extension of the work in [24], which examined the $\mathcal{H}_2$ performance of RSNs and described a topology synthesis procedure based on results from combinatorial optimization. In this work, we consider a graph-centric characterization of the system $\mathcal{H}_\infty$ performance of RSNs for both analysis and synthesis purposes. A distinction is made between RSNs with homogeneous agent dynamics and RSNs with heterogeneous agent dynamics. Although homogeneous RSNs can be considered a subset of heterogeneous RSNs, it is more illuminating to consider these cases separately due to the algebraic simplicity of the former case. Understanding how properties of the interconnection graph leads to improvements in system performance can give insight into the design of sensing topologies. In particular, we consider how characterization of the $\mathcal{H}_\infty$ performance leads to a robust topology design formulation.

The paper is organized as follows. Section §I-A provides our notational conventions and a brief overview of notions from algebraic graph theory. In section §II, general models for homogeneous and heterogeneous RSNs are developed. Section §III derives expressions for the $\mathcal{H}_\infty$ norms of homogeneous and heterogeneous RSNs, with an emphasis given to the role of the underlying topology. Section §IV presents a synthesis formulation for the robust topology design of RSNs. Finally, section §V offers some concluding remarks on this work.

A. Preliminaries and Notations

We provide some mathematical preliminaries and notations here. Matrices are denoted by capital letters (e.g., A), and vectors by lower case letters (e.g., x). Diagonal matrices will be written as $D = \mathbf{diag}\{d_1, \ldots, d_n\}$; this notation will also be employed for block-diagonal matrices and linear operators. A matrix and/or a vector that consists of all zero entries will be denoted by $\mathbf{0}$; whereas, '0' will simply denote the scalar zero. Similarly, the vector $\mathbf{1}$ denotes the vector of all ones, and $\mathbf{J} = \mathbf{1}\mathbf{1}^T$. The $n \times n$ identity matrix is denoted as I_n; we also append a subscript to $\mathbf{J}$, $\mathbf{1}$, and $\mathbf{0}$ to denote its dimension when it is not clear. The set of real numbers will be denoted as $\mathbb{R}$, and $\| \, . \, \|$ denotes the standard 2-norm for vectors and matrices; on the other hand, for m-

[†]D. Zelazo is with the Institute for Systems Theory and Automatic Control at the University of Stuttgart, Pfaffenwaldring 9, 70569 Stuttgart, Germany; Email: *daniel.zelazo@ist.uni-stuttgart.de*. [‡] M. Mesbahi is with the Department of Aeronautics and Astronautics, University of Washington, Box 352400, Seattle, WA 98195-2400; Email: *mesbahi@aa.washington.edu*

978-1-4244-7427-1/10/$26.00 ©2010 AACC

dimensional finite energy signals, that is signals in the space $\mathcal{L}_2^m$, the norm is induced by the inner-product and denoted as $\|u(j\omega)\|_{\mathcal{L}_2}^2 = \langle u(j\omega), u(j\omega)\rangle = \int_{-\infty}^{\infty} u(j\omega)^* u(j\omega) d\omega$. The $\mathcal{H}_2$ and $\mathcal{H}_\infty$ norms for linear operators will be denoted as $\|\,.\,\|_2$ and $\|\,.\,\|_\infty$. The adjoint of a linear operator f is denoted by f^*. The Kronecker product of two matrices A and B is written as $A \otimes B$ [13].

Graphs and the matrices associated with them will be widely used in this work. The reader is referred to [10] for a detailed treatment of the subject and we present here only a minimal summary of relevant constructs and results. An undirected (simple) graph $\mathcal{G}$ is specified by a vertex set $\mathcal{V}$ and an edge set $\mathcal{E}$ whose elements characterize the incidence relation between distinct pairs of $\mathcal{V}$. Two vertices i and j are called *adjacent* (or neighbors) when $\{i, j\} \in \mathcal{E}$; we denote this by writing $i \sim j$. The cardinalities of the vertex and edge sets of $\mathcal{G}$ will be denoted by $|\mathcal{V}|$ and $|\mathcal{E}|$, respectively. An *orientation* of an undirected graph $\mathcal{G}$ is the assignment of directions to its edges, i.e., an edge e_k is an ordered pair (i, j) such that i and j are, respectively, the initial and the terminal nodes of e_k.

In this work we make extensive use of the $|\mathcal{V}| \times |\mathcal{E}|$ incidence matrix, $E(\mathcal{G})$, for a graph with arbitrary orientation. The incidence matrix is a $\{0, \pm 1\}$-matrix with rows and columns indexed by the vertices and edges of $\mathcal{G}$ such that $[E(\mathcal{G})]_{ik}$ has the value '+1' if node i is the initial node of edge e_k, '-1' if it is the terminal node, and '0' otherwise. The degree of vertex i, d_i, is the cardinality of the set of vertices adjacent to it; we define the degree matrix as $\Delta(\mathcal{G}) = \mathbf{diag}\{d_1, \ldots, d_{|\mathcal{V}|}\}$. The adjacency matrix of a graph, $A(\mathcal{G})$, is the symmetric $|\mathcal{V}| \times |\mathcal{V}|$ matrix such that $[A(\mathcal{G})]_{ij}$ takes the value '+1' if node i is connected to node j, and '0' otherwise.

The (graph) Laplacian of $\mathcal{G}$,

$$L(\mathcal{G}) \;:=\; E(\mathcal{G})E(\mathcal{G})^T \;=\; \Delta(\mathcal{G}) - A(\mathcal{G}), \qquad (1)$$

is a rank deficient positive semi-definite matrix. The eigenvalues of the graph Laplacian are real and will be ordered and denoted as $0 = \lambda_1(\mathcal{G}) \leq \lambda_2(\mathcal{G}) \leq \cdots \leq \lambda_{|\mathcal{V}|}(\mathcal{G})$.

In order to apply the framework developed in this paper to specific graphs, we will work with the complete graph and its generalization in terms of k-regular graphs, which are defined as follows. The *complete graph* on n nodes, K_n, is the graph where all possible pairs of vertices are adjacent, or equivalently, if the degree of all vertices is $|\,\mathcal{V}\,| - 1$. Figure 1(a) depicts K_{10}, the complete graph on 10 nodes. When every node in a graph with n nodes has the same degree $k \leq n-1$, it is called a k-regular graph. Figure 1(b) shows a 4-regular graph.

II. RELATIVE SENSING NETWORK MODEL

In this section we derive a general plant model for relative sensing networks. An RSN, in its most general setting, is comprised of individual sensing agents which, for this work, are assumed to contain linear and time-invariant dynamics. The agents are coupled to other agents through their sensed outputs; the output coupling is defined

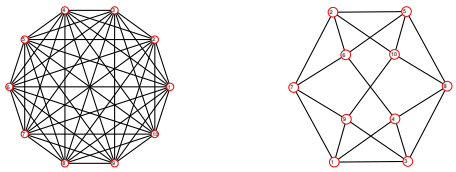

(a) K_{10} Graph (b) A 4-regular Graph

Fig. 1. Example of regular graphs.

by the connection topology describing their interactions. We identify two classes of RSNs in this paper: 1) homogeneous RSNs and 2) heterogeneous RSNs. For both cases, we will work with a group of n dynamic systems (the "agents"), with state-space representation

$$\Sigma_i : \begin{cases} \dot{x}_i(t) = A_i x_i(t) + B_i u_i(t) + \Gamma_i w_i(t) \\ z_i(t) = C_i^z x_i(t) + D_i^{zu} u_i(t) + D_i^{zw} w_i(t) \\ y_i(t) = C_i^y x_i(t) + D_i^{yw} w_i(t), \end{cases} \qquad (2)$$

where each agent is indexed by the sub-script i. Here, $x_i(t)$ represents the state, $u_i(t)$ the control, $w_i(t)$ an exogenous input (e.g., disturbances and noises), $z_i(t)$ the controlled variable, and $y_i(t)$ the locally measured output.

We denote the transfer-function representation of Σ_i as $\hat{\Sigma}_i$,

$$\begin{bmatrix} Z_i(s) \\ Y_i(s) \end{bmatrix} = \begin{bmatrix} H_i^{zu}(s) & H_i^{zw}(s) \\ H_i^{yu}(s) & H_i^{yw}(s) \end{bmatrix} \begin{bmatrix} U_i(s) \\ W_i(s) \end{bmatrix} = \hat{\Sigma}_i \begin{bmatrix} U_i(s) \\ W_i(s) \end{bmatrix}, \qquad (3)$$

with

$$\begin{aligned} H_i^{zu}(s) &= C_i^z (sI - A_i)^{-1} B_i + D_i^{zu}, \\ H_i^{zw}(s) &= C_i^z (sI - A_i)^{-1} \Gamma_i + D_i^{zw}, \\ H_i^{yu}(s) &= C_i^y (sI - A_i)^{-1} B_i, \\ H_i^{yw}(s) &= C_i^y (sI - A_i)^{-1} \Gamma_i + D_i^{yw}. \end{aligned}$$

In the homogeneous case, it is assumed that each dynamic agent in the RSN is described by the same set of linear state-space dynamics (e.g., $\Sigma_i = \Sigma_j$ for all i, j). When working with homogeneous RSN, we drop the sub-script for all state-space and operator representations of the system. We will also assume no feedforward terms of the control to the measured output. Additionally, we assume a minimal realization for each agent with compatible outputs for all agents, e.g., system outputs will correspond to the same physical quantity. It should be noted that in a heterogeneous system, the dimension of each agent need not be the same; however, using a "padding argument," it can be assumed that all agents have identical dimensions for their respective state space.

The parallel interconnection of all the agents has a state-space description

$$\begin{aligned} \dot{\mathbf{x}}(t) &= \mathbf{A}\mathbf{x}(\mathbf{t}) + \mathbf{B}\mathbf{u}(\mathbf{t}) + \mathbf{\Gamma}\mathbf{w}(\mathbf{t}) \\ \mathbf{z}(t) &= \mathbf{C}^{\mathbf{z}}\mathbf{x}(\mathbf{t}) + \mathbf{D}^{\mathbf{zu}}\mathbf{u}(\mathbf{t}) + \mathbf{D}^{\mathbf{zw}}\mathbf{w}(\mathbf{t}) \\ \mathbf{y}(t) &= \mathbf{C}^{\mathbf{y}}\mathbf{x}(\mathbf{t}) + \mathbf{D}^{\mathbf{yw}}\mathbf{w}(\mathbf{t}), \end{aligned} \qquad (4)$$

with $\mathbf{x}(t)$, $\mathbf{u}(t)$, $\mathbf{w}(t)$, $\mathbf{z}(t)$, and $\mathbf{y}(t)$ denoting respectively, the concatenated state vector, control vector, exogenous input

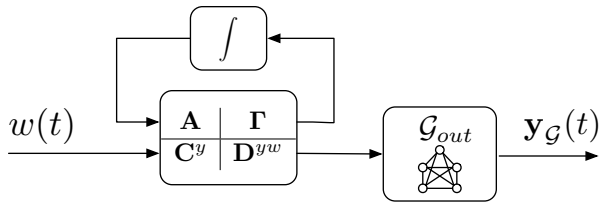

Fig. 2. Global RSN layer block diagram; the feedback connection represents an upper fractional transformation [7].

vector, controlled vector, and output vector of all the agents in the RSN. The bold faced matrices represent the block diagonal aggregation of each agent's state-space matrices, e.g., $\mathbf{A} = \mathbf{diag}\{A_1, \ldots, A_n\}$.

The global RSN layer we examine in this paper is motivated by the relative sensing problem. The sensed output of the RSN is the vector $\mathbf{y}_{\mathcal{G}}(t)$ containing relative state information of each agent and its neighbors. The incidence matrix of a graph naturally captures state differences and will be the algebraic construct used to define the relative outputs of RSNs. For example, the output sensed between agent i and agent j would be of the form $y_i(t) - y_j(t)$. This can be compactly written using the incidence matrix for the entire RSN as

$$\mathbf{y}_{\mathcal{G}}(t) = (E(\mathcal{G})^T \otimes I)\mathbf{y}(t). \tag{5}$$

Here, $\mathcal{G}$ is the graph that describes the connection topology of the RSN; the node set is given as $\mathcal{V} = \{1, \ldots, n\}$. The global layer can be visualized as in the block diagram shown in Figure 2.

When considering the analysis of the global layer, we are interested in studying the map from the agent's exogenous inputs to the RSN sensed output. Using the above notations we can express the heterogeneous RSN in a compact form,

$$\Sigma_{het}(\mathcal{G}) : \begin{cases} \dot{\mathbf{x}}(t) &= \mathbf{A}\mathbf{x}(t) + \mathbf{B}\mathbf{u}(t) + \mathbf{\Gamma}\mathbf{w}(t) \\ \mathbf{z}(t) &= \mathbf{C}^z\mathbf{x}(t) + \mathbf{D}^{zu}\mathbf{u}(t) + \mathbf{D}^{zw}\mathbf{w}(t) \\ \mathbf{y}(t) &= \mathbf{C}^y\mathbf{x}(t) + \mathbf{D}^{yw}\mathbf{w}(t) \\ \mathbf{y}_{\mathcal{G}}(t) &= (E(\mathcal{G})^T \otimes I)\mathbf{C}^y\mathbf{x}(t) \end{cases} \tag{6}$$

The homogeneous RSN, $\Sigma_{hom}(\mathcal{G})$, can be expressed using the Kronecker product. For example, $\mathbf{A} = I \otimes A$ and $(E(\mathcal{G})^T \otimes I)\mathbf{C}^y = E(\mathcal{G})^T \otimes C^y$.

Similarly, the transfer function representation is written as

$$\hat{\Sigma}_{het} = \begin{bmatrix} \mathbf{H}^{zu}(s) & \mathbf{H}^{zw}(s) \\ \mathbf{H}^{yu}(s) & \mathbf{H}^{yw}(s) \\ (E(\mathcal{G})^T \otimes I)\,\mathbf{H}^{yu}(s) & (E(\mathcal{G})^T \otimes I)\,\mathbf{H}^{yw}(s) \end{bmatrix}, \tag{7}$$

where, as in the state space model, bold faced transfer functions denotes the block diagonal aggregation of each agent's corresponding transfer function, e.g., $\mathbf{H}^{zu}(s) = \mathbf{diag}\{H_1^{zu}(s), \ldots, H_n^{zu}(s)\}$. The homogeneous system, $\hat{\Sigma}_{hom}$, can also be written using the Kronecker product in a similar manner as described above.

For notational simplicity, we denote $T_{hom}^{w\mapsto\mathcal{G}}$ and $T_{het}^{w\mapsto\mathcal{G}}$ as the map from the exogenous inputs to the RSN sensed output for homogeneous and heterogeneous systems respectively, e.g., $T_{hom}^{w\mapsto\mathcal{G}} = E(\mathcal{G})^T \otimes H^{yw}(s)$. We also use transfer function and state-space representations interchangeably noting the appropriate realization can be inferred by context. For example, H_i^{yw} will be used to represent both the state-space and transfer function representation of the open-loop map from the exogenous inputs to the measurement of agent i.

III. GRAPH THEORETIC BOUNDS ON $\mathcal{H}_\infty$ PERFORMANCE

In this section we explore a graph-theoretic characterization of the $\mathcal{H}_\infty$ performance of the RSN model presented in §II. The main goal is to highlight the role of the underlying connection topology on the system norms mapping the exogenous inputs $\mathbf{w}(t)$ to the relative sensed output $\mathbf{y}_{\mathcal{G}}(t)$, $T^{w\mapsto\mathcal{G}}$. We assume that the observation matrix for the sensed output is the same as for the local measurement; that is $\mathbf{C} = \mathbf{C}^y$ and $\mathbf{H}^{\mathcal{G}w} = \mathbf{H}^{yw}$, as in (6) and (7). Additionally, we assume throughout this section that the underlying connection graph $\mathcal{G}$ is connected and $\mathcal{V} = \{1, \ldots, n\}$. For analysis, we finally assume that each agent has stable dynamics.

We first recall that the $\mathcal{H}_\infty$ norm for a dynamic system captures how a measurable signal with finite energy, i.e., a signal in $\mathcal{L}_2$, is amplified at the monitored output of the system. Moreover, this norm has implications for robustness, disturbance rejection, and uncertainty management for dynamic systems. Specifically, the $\mathcal{H}_\infty$ norm of a linear system with transfer-function representation $H(s)$ is characterized as

$$\begin{aligned} \|H(j\omega)\|_\infty &= \sup_\omega \{\overline{\sigma}\,[H(j\omega)]\} \\ &= \sup_{\|U(j\omega)\|_2=1} \|H(j\omega)U(j\omega)\|_{\mathcal{L}_2}, \end{aligned} \tag{8}$$

where $\overline{\sigma}[A]$ denotes the largest singular value of the matrix A. The induced-norm description allows us to state the sub-multiplicative property of the $\mathcal{H}_\infty$ norm for two operators as $\|H(j\omega)P(j\omega)\|_\infty \leq \|H(j\omega)\|_\infty \|P(j\omega)\|_\infty$.

In the context of RSNs, therefore, *the $\mathcal{H}_\infty$ system norm can be used to capture how disturbances and finite energy exogenous signals, including reference signals, result in the asymptotic deviation of the sensed output of the network.* This section aims to explicitly characterize the effect of the network on the $\mathcal{H}_\infty$ norm of the system. We separate our analysis into the homogeneous and heterogeneous cases.

A. Homogeneous RSN $\mathcal{H}_\infty$ Performance

Given the transfer function representation of the homogeneous RSN in (7), we can write the map from the disturbances to the networked output as

$$\mathbf{Y}_{\mathcal{G}}(s) = \left(E(\mathcal{G})^T \otimes H^{yw}\right)\mathbf{U}(s). \tag{9}$$

Theorem 3.1: The $\mathcal{H}_\infty$ norm of the homogeneous RSN (6) is given as

$$\left\|T_{hom}^{w\mapsto\mathcal{G}}\right\|_\infty = \|E(\mathcal{G})\|\,\|H^{yw}\|_\infty. \tag{10}$$

Proof: The norm expression follows directly from the definition in (8) and the Kronecker product property [**?**]

$$\|A \otimes B\| = \|A\|\|B\|. \tag{11}$$

■

The expression (10) states that the overall $\mathcal{L}_2$ gain of the system is proportional to the matrix 2-norm of the incidence matrix. In fact, since $\|E(\mathcal{G})\| = \sqrt{\|L(\mathcal{G})\|} = \lambda_n^{1/2}$, the behavior of the largest eigenvalue of the graph Laplacian is of particular interest. Moreover, an important observation is that certain graph structures will naturally lead to a smaller $\mathcal{H}_\infty$ norm. If we restrict our topology to spanning trees we can state stronger a set of results.

Corollary 3.2: When the underlying topology is a spanning tree, the path graph is the topology resulting in the smallest $\mathcal{H}_\infty$ norm for the homogeneous RSN (6). Moreover, the star graph is the topology resulting in the largest $\mathcal{H}_\infty$ norm for the homogeneous (6) among all spanning trees.

Proof: In [18] it was shown that the path graph has the smallest spectral norm for the graph Laplacian among all spanning trees. In [11] it was shown that the star graph has the largest spectral norm for the graph Laplacian among all spanning trees. ■

B. Bounds on the Heterogeneous RSN $\mathcal{H}_\infty$ Performance

We follow a similar procedure for the heterogeneous case. Using the transfer function representation of the heterogeneous RSN in (7) we can write the map from the disturbances to the networked output as

$$\mathbf{Y}_{\mathcal{G}}(s) \quad = \quad \left(E(\mathcal{G})^T \otimes I\right) \mathbf{H}^{yw}(s)\mathbf{U}(s). \tag{12}$$

Calculating the $\mathcal{H}_\infty$ norm involves finding the singular values of the transfer function

$$T_{het}^{w\mapsto\mathcal{G}} \quad = \quad \left(E(\mathcal{G})^T \otimes I\right) \mathbf{H}^{yw}(s). \tag{13}$$

In general, an analytic expression for the singular values of the system in (13) is difficult to obtain. However, it is possible to generate bounds on the system-norm, leading to the following result.

Theorem 3.3: The $\mathcal{H}_\infty$ norm of the homogeneous RSN (6) is bounded as

$$\|T_{het}^{w\mapsto\mathcal{G}}\|_\infty \leq \|E(\mathcal{G})^T Q\| \leq \left\|E(\mathcal{G})^T\right\| \max_i \|H_i^{yw}\|_\infty, \tag{14}$$

where $Q = \mathbf{diag}\{\|H_1^{yw}\|_\infty, \ldots, \|H_n^{yw}\|_\infty\}$.

Proof: The upper-bound immediately arises from the sub-multiplicative property of the matrix 2-norm as $\|E(\mathcal{G})^T Q\| \leq \|E(\mathcal{G})^T\|\|Q\|$. Since Q is a diagonal matrix we conclude that $\|Q\| = \max_i \|H_i^{yw}\|_\infty$. To show the lower-bound we follow the following chain of inequalities as

$$\begin{aligned}
\|T_{het}^{w\mapsto\mathcal{G}}\|_\infty^2 &= \sup_{\|U(j\omega)\|_{\mathcal{L}_2}=1} \|(E(\mathcal{G})^T \otimes I)\mathbf{H}^{yw}(j\omega)U(j\omega)\|_{\mathcal{L}_2}^2 \\
&= \sup_{\|U\|_{\mathcal{L}_2}=1} \int_{-\infty}^{\infty} U^*(\mathbf{H}^{yw})^* \left(L(\mathcal{G}) \otimes I\right) \mathbf{H}^{yw} U d\omega \\
&= \sup_{\|U\|_{\mathcal{L}_2}=1} \int_{-\infty}^{\infty} \mathbf{Tr}[UU^*(\mathbf{H}^{yw})^* \left(L(\mathcal{G}) \otimes I\right) \mathbf{H}^{yw}] d\omega \\
&\leq \sup_{\|U\|_{\mathcal{L}_2}=1} \int_{-\infty}^{\infty} \mathbf{Tr}(U^*)\mathbf{Tr}[(\mathbf{H}^{yw})^* \left(L(\mathcal{G}) \otimes I\right) \mathbf{H}^{yw}] d\omega \\
&\leq \|QE(\mathcal{G})\|,
\end{aligned} \tag{15}$$

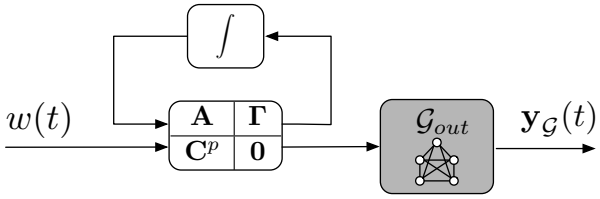

Fig. 3. Topology design; the feedback connection represents an upper fractional transformation [7].

where the second to last inequality follows from the property that for Hermitian matrices, M and N, $\mathbf{Tr}[MN] \leq \mathbf{Tr}[M]\mathbf{Tr}[N]$, and the last identity follows from the property that the positive-definite ordering $\mathbf{H}^{yw}(j\omega)^*(L(\mathcal{G}) \otimes I)\mathbf{H}^{yw}(j\omega) \leq (Q \otimes I)(L(\mathcal{G}) \otimes I)(Q \otimes I)$ holds for all ω. ■

Corollary 3.4: When each agent in (6) is a single-input single-output (SISO) system, the norm bound in (14) is tight.

An interesting implication of the norm bounds developed in the proof relates the $\mathcal{L}_2$ gain of a heterogeneous RSN to that of a homogeneous RSN. Consider an ordering of each agent in a heterogeneous RSN by the value of the $\mathcal{H}_\infty$ norm of each agent,

$$\|H_{k(1)}^{yw}\|_\infty \leq \cdots \leq \|H_{k(n)}^{yw}\|_\infty, \tag{16}$$

where $k : \{1, \ldots, n\} \mapsto \{1, \ldots, n\}$ maps the old index set to the norm-ordered one. The $\mathcal{H}_\infty$ norm of the heterogeneous system $T_{het}^{w\mapsto\mathcal{G}}$ can be bounded from above and below by homogeneous systems as

$$\|E(\mathcal{G})\|\|H_{k(1)}^{yw}\|_\infty \leq \|T_{het}^{w\mapsto\mathcal{G}}\|_\infty \leq \|E(\mathcal{G})\|\|H_{k(n)}^{yw}\|_\infty.$$

This inequality suggests that in addition to the structure of the underlying topology, one can consider the dynamic differences between agents as an important factor in the performance of the overall system.

IV. ROBUST SYNTHESIS OF RSN

We now consider the synthesis of the underlying connection topology, as shown in Figure 3. As we are only considering the topology, we use the following heterogeneous state-space model for the RSN,

$$T_{het}^{w\mapsto\mathcal{G}} \quad : \quad \left\{ \begin{array}{rcl} \dot{\mathbf{x}}(t) & = & \mathbf{A}\mathbf{x}(t) + \mathbf{\Gamma}\mathbf{w}(t) \\ \mathbf{y}_{\mathcal{G}}(t) & = & \left(E(\mathcal{G})^T \otimes C_p\right)\mathbf{x}(t) \end{array} \right. . \tag{17}$$

We would like to find topologies that minimize the effect of disturbances entering each agent on the relative sensed output of the entire system, that is minimizing the performance objective $\|T_{het}^{w\mapsto\mathcal{G}}\|_\infty$. This can be considered a problem in combinatorial optimization [14], as the decision to include an edge in the graph is binary. The general synthesis problem can be written as

$$\begin{array}{ll} \min\limits_{\mathcal{G}} & \|T_{het}^{w\mapsto\mathcal{G}}\|_\infty \\ \text{s.t.} & \mathcal{G} \text{ is connected.} \end{array} \tag{18}$$

The challenge, therefore, is to find numerically tractable algorithms to solve (18). In what follows, we solve a variation of (18) that minimizes the robust performance of a weighted version of (17) with uncertainty on the edge weights.

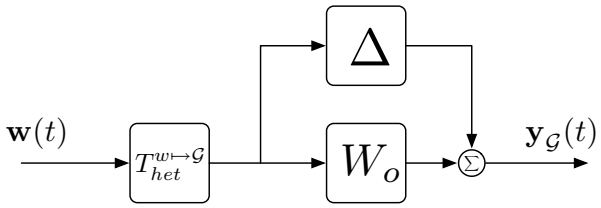

Fig. 4. Multiplicative uncertainty for NDS

Motivated by the results of §III, we find that (18) reduces to the minimization of the spectral norm of the weighted incidence matrix, $\|QE(\mathcal{G})\|$, where Q was defined in Theorem 3.3. Minimization of this objective can be formulated as a mixed-integer semi-definite program. For reasonably sized problem instances this can be solved using, for example, branch-and-bound algorithms [14].

While topology design is an important application, the $\mathcal{H}_\infty$ framework allows us to consider the robustness of certain topologies. In this direction, we consider a variation of (18) that aims to minimize the *robust performance* of the RSN in (17). For such an analysis, we adjust the RSN model to allow for uncertainty in the sensing protocol. Specifically, we introduce the notion of a weighted edge for the sensed output. This model might be used to capture the fidelity of a relative measurement.

$$T_{het}^{w\mapsto\mathcal{G}}(W_o) \ : \left\{ \begin{array}{rcl} \dot{\mathbf{x}}(t) & = & \mathbf{A}\mathbf{x}(t)+\mathbf{\Gamma}\mathbf{w}(t) \\ \mathbf{y}_{\mathcal{G}}(t) & = & \left(W_o E(\mathcal{G})^T \otimes C_p\right)\mathbf{x}(t). \end{array} \right. \quad (19)$$

In (19), each diagonal entry of $W_o = \mathbf{diag}\{w_1,\ldots,w_{|\mathcal{E}|}\}$ represents the nominal weights on each edge in the graph. A weight of zero corresponds to the absence of an edge. We will also assume all the weights are non-negative. The model (19) relates to (17) through the output as $T_{het}^{w\mapsto\mathcal{G}}(W_o) = (W_o\otimes I)T_{het}^{w\mapsto\mathcal{G}}$.

Using (19), we can introduce a structured uncertainty on each edge weight. The uncertainty set is defined as

$$\mathbf{\Delta} \ = \ \{\text{diag}\{\delta_1,\ldots,\delta_{|\mathcal{E}|}\} \ : \delta_i\in\mathbb{R},\ |\delta_i|\le 1\}. \quad (20)$$

The true edge weight can thus be written as $W = W_o+\Delta$, for $\Delta\in\mathbf{\Delta}_w$. This can be considered as an output-multiplicative uncertainty, as shown in Figure 4.

The problem (18) can now be restated as the *robust optimization* problem [4],

$$\begin{array}{lll} \min\limits_{W_o} & \max_{\|\mathbf{\Delta}\|\le 1} & \|QE(\mathcal{G})\left(W_o+\mathbf{\Delta}\right)\| \\ \text{s.t.} & & \mathcal{G} \text{ is connected in the presence} \\ & & \text{of edge weight uncertainty.} \end{array} \quad (21)$$

This problem can be solved as a semi-definite program, the procedure of which is outlined in [4]. To apply these results, we must express the objective and constraints of (21) as a perturbed LMI in the form,

$$F(x,\delta) \ = \ F_0(x)+\sum_{i=1}^{l}\delta_i F_i(x), \quad (22)$$

where each $F_i(x)$ is a symmetric matrix and affine in the variable x.

First, we scalarize the objective function by introducing a new variable γ and noting that $\|QE(\mathcal{G})\left(W_o+\mathbf{\Delta}\right)\|\le\gamma$ can be written (via the Schur complement) as the LMI

$$\left[\begin{array}{cc} \gamma I & QE(\mathcal{G})(W_o+\mathbf{\Delta}) \\ (W_o+\mathbf{\Delta})E(\mathcal{G}^TQ & I \end{array}\right] \ge 0. \quad (23)$$

Defining the matrices $S_i\in\mathbb{R}^{|\mathcal{E}|\times|\mathcal{E}|}$ and $V(\gamma)$ as

$$[S_i]_{kl} = \left\{\begin{array}{ll} 1 & k=l=i \\ 0 & \text{otherwise} \end{array}\right. , \ V(\gamma) = \left[\begin{array}{cc} \gamma I & \mathbf{0} \\ \mathbf{0} & I \end{array}\right], \quad (24)$$

we can express (23) in the form (22) as

$$F_1(w,\delta) = V(\gamma)+\sum_{i=1}^{|\mathcal{E}|}(w_i+\delta_i)\left[\begin{array}{cc} \mathbf{0} & QE(\mathcal{G})S_i \\ S_iE(\mathcal{G})^TQ & \mathbf{0} \end{array}\right] \ge 0. \quad (25)$$

Similarly, the robust connectivity constraint can also be expressed in the form (22). Recall that for a connected graph, $\lambda_2(\mathcal{G})>0$, and the eigenvector associated with $\lambda_1(\mathcal{G})=0$ is the vector of all ones, $\mathbf{1}$. Defining the matrix P such that $\mathbf{IM}\{P\} = \mathbf{span}\{\mathbf{1}^\perp\}$, we obtain

$$F_2(w,\delta) = \sum_{i=1}^{|\mathcal{E}|}(w_i+\delta_i)P^T(e_ie_i^T)P \ > \ 0. \quad (26)$$

Using (25) and (26) we define

$$F_0^1(w) \ = \ \left[\begin{array}{cc} \gamma I & QE(\mathcal{G})W_o \\ W_oE(\mathcal{G})^TQ & I \end{array}\right], \quad (27)$$

$$F_0^2(w) \ = \ P^TE(\mathcal{G})W_oE(\mathcal{G})^TP, \quad (28)$$

$$F_i^1 = \left[\begin{array}{cc} \mathbf{0} & QE(\mathcal{G})S_i \\ S_iE(\mathcal{G})^TQ & \mathbf{0} \end{array}\right] \ , \ \ F_i^2 = P^Te_ie_i^TP. \quad (29)$$

The expressions in (27) and (29) can now be applied to the results in [**?**] to obtain the following SDP,

$$\begin{array}{lll} \min\limits_{w,S_i,T_i} & \gamma & \quad (30) \\ \text{s.t.} & \left[\begin{array}{cccc} S_i & F_1^i & \cdots & F_{|\mathcal{E}|}^i \\ F_1^i & T_i & & \\ \vdots & & \ddots & \\ F_{|\mathcal{E}|}^i & & & T_i \end{array}\right] \ge 0 \ , \ i=1,2 & \\ & S_i+T_i\le 2F_0^i \ , \ i=1,2 \ , \ \sum\limits_i w_i=\alpha, & \\ & 0\le w_i\le w_{max} \ , \ i=1,\ldots,|\mathcal{E}| & \end{array}$$

where the last constraints constrain the aggregate edge weight sum and edge weight range.

To illustrate this procedure, we consider an RSN with $n=10$ heterogeneous and SISO systems (generated randomly in MATLAB). The input graph is the complete graph, K_n, allowing the program in (30) to select the optimal weights on every possible edge combination. For $\alpha=n-1$ and $w_{max}=2$, (30) was solved using SeDuMi in Matlab. The resulting topology is shown in Figure 5. Note that every edge has a

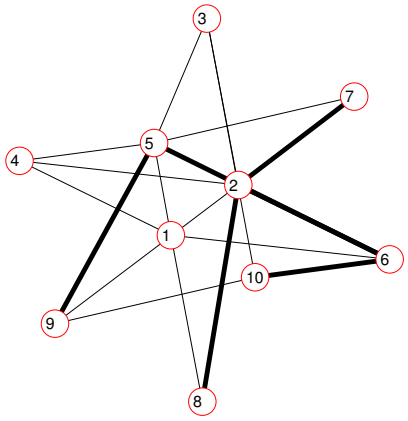

Fig. 5. Optimal topology

positive weight, however, only edges with $w_i > 0.1$ were drawn. The thickness of the line indicates a larger weight.

Remark 4.1: While the problem formulation presented above is concerned with static edge weight uncertainty, the principle can be extended to include dynamic edge weights. For example, each relative sensor may be characterized by a frequency dependent weight, $w_i(s)$, and the corresponding uncertainty can be considered as an unstructured norm-bounded uncertainty.

Remark 4.2: The SDP (30) presents an analytic framework for solving the robust topology design problem. However, it should be noted that due to the auxiliary variables defined, the size of this problem can grow very large with the number of nodes (for the complete graph on n nodes, there are $n(n-1)/2$ edges). While interior-point methods offer polynomial-time algorithms, for excessively large problem instances (30) might lead to numerical problems. This points to the need to consider specialized solution methods or alternative problem formulations.

V. CONCLUSIONS

This paper focused on the development of graph theoretic performance bounds and synthesis techniques for distinct classes of relative sensing networks (RSN). The results of this paper highlight an important connection between certain graph-theoretic concepts and systems-theoretic properties. In particular, the $\mathcal{H}_\infty$ performance depends on the spectral norm of a node-weighted incidence matrix, which is strongly dependent on the actual structure of the graph.

Synthesis methods for RSNs were also presented. Using methods from robust semidefinite programming, a synthesis procedure was then developed that aims to minimize the $\mathcal{H}_\infty$ performance of an RSN with uncertainty on the edge weights. This work also suggests that the relationship between systems-theoretic properties and graph properties in RSNs can be examined further in the systems and control community. In fact, we believe that developing efficient solution methods for the synthesis of such systems will involve further interpreting results from graph theory and combinatorial optimization in a system-theoretic context.

ACKNOWLEDGMENTS

The research of the authors was sponsored by NSF grant ECCS-0501606.

REFERENCES

[1] I.F. Akyildiz, Y. Sankarasubramaniam, and E. Cayirci. A survey on sensor networks. *IEEE Communications Magazine*, 40(8):102–114, 2002.

[2] P. Barooah, N. Machado Da Silva, and J.P. Hespanha. *Distributed Optimal Estimation from Relative Measurements for Localization and Time Synchronization*, volume 4026 of *Lecture Notes in Computer Science*, chapter 17, pages 266–281. Springer-Verlag, Berlin/Heidelberg, 2006.

[3] A. Behar, J. Matthews, F. Carsey, and J. Jones. NASA/JPL Tumbleweed polar rover. In *2004 IEEE Aerospace Conference Proceedings (IEEE Cat. No.04TH8720)*, pages 388–395. IEEE, 2004.

[4] A. Ben-tal, L. El Ghaoui, and A. Nemirovski. *Robust semidefinite programming*, chapter 6. Springer-Verlag, New York, 2000.

[5] G. Chen and Z. Duan. Network synchronizability analysis: a graph-theoretic approach. *Chaos (Woodbury, N.Y.)*, 18(3):037102, 2008.

[6] K. Danzmann and LISA Study Team. LISA: Laser Interferometer Space Antenna for the Detection and Observation of Gravitational Waves, 1998.

[7] G.E. Dullerud and F. Paganini. *A course in robust control theory: a convex approach*. Springer-Verlag, New York, 2000.

[8] J.A. Fax and R.M. Murray. Information Flow and Cooperative Control of Vehicle Formations. *IEEE Transactions on Automatic Control*, 49(9):1465–1476, September 2004.

[9] C. Fridlund. Infrared space interferometry the DARWIN mission. *Advances in Space Research*, 30(9):2135–2145, 2002.

[10] C.D. Godsil and G. Royle. *Algebraic graph theory*. Springer, 2001.

[11] I. Gutman. The star is the tree with greatest greatest Laplacian eigenvalue. *Kragujevac J. Math*, 24:61–65, 2002.

[12] F.Y. Hadaegh and R.S. Smith. Control of Deep-Space Formation-Flying Spacecraft; Relative Sensing and Switched Information. *Journal of Guidance, Control, and Dynamics*, 28(1):106–114, January 2005.

[13] R.A. Horn and C.R. Johnson. *Topics in Matrix Analysis*. Cambridge University Press, New York, NY, 1991.

[14] B.H. Korte and J. Vygen. *Combinatorial optimization: theory and algorithms*. Springer-Verlag, Berlin, 2000.

[15] P.R. Lawarence. The Terrestrial Planet Finder. In *Proceedings of the IEEE Aerospace Conference*.

[16] M. Mesbahi and F.Y. Hadaegh. Formation flying control of multiple spacecraft via graphs, matrix inequalities, and switching. In *Proceedings of the 1999 IEEE International Conference on Control Applications*, pages 1211–1216. Ieee, 1999.

[17] R. Olfati-Saber. Distributed Kalman Filter with Embedded Consensus Filters. In *Proceedings of the 44th IEEE Conference on Decision and Control*, pages 8179–8184. Ieee, 2005.

[18] M. Petrovic and I. Gutman. The path is the tree with smallest greatest Laplacian eigenvalue. *Kragujevac J. Math*, 24:67–70, 2002.

[19] A. Rahmani, M. Ji, M. Mesbahi, and M. Egerstedt. Controllability of multiagent systems: from a graph-theoretic perspective. *SIAM Journal on Control and Optimization*, 48(1):162, 2008.

[20] J. Sandhu, M. Mesbahi, and T. Tsukamaki. Relative sensing networks: observability, estimation, and the control structure. *44th IEEE Conference on Decision and Control, 2005 ...*, 2005.

[21] G. Sholomitsky, O. Prilutsky, and V. Rodin. Infrared Space Interferometer, 1977.

[22] D. Zelazo and M. Mesbahi. On the observability properties of homogeneous and heterogeneous networked dynamic systems. In *2008 47th IEEE Conference on Decision and Control*, pages 2997–3002. IEEE, December 2008.

[23] D. Zelazo and M. Mesbahi. Edge Agreement: Graph-Theoretic Performance Bounds and Passivity Analysis. *IEEE Transactions on Automatic Control (to appear)*, 2009.

[24] D. Zelazo and M. Mesbahi. $\mathcal{H}_2$ Performance of Relative Sensing Networks: Analysis and Synthesis. In *AIAA Infotech@Aerospace Conference and AIAA Unmanned...Unlimited Conference*, volume 21, pages C3–C3, Seattle, WA, April 2009.